
LEARNING LOCAL COMPLEX FEATURES USING RANDOMIZED NEURAL NETWORKS FOR TEXTURE ANALYSIS

Lucas C. Ribas¹, Leonardo F. S. Scabini², Jarbas Joaci de Mesquita Sá Junior³, and Odemir M. Bruno^{1,2}

¹São Carlos Institute of Physics, University of São Paulo (USP), PO Box 369, 13560-970, São Carlos, SP, Brazil.
Scientific Computing Group

²Institute of Mathematics and Computer Science, University of São Paulo (USP), USP, Avenida Trabalhador São-Carlense, 400, 13566-590, São Carlos, SP, Brazil.

³Curso de Engenharia da Computação, Programa de Pós-Grad. em Eng. Elétrica e de Computação, Campus de Sobral, Universidade Federal do Ceará, Rua Coronel Estanislau Frota, 563, Centro, Sobral, Ceará, CEP: 62010-560, Brasil

ABSTRACT

Texture is a visual attribute largely used in many problems of image analysis. Currently, many methods that use learning techniques have been proposed for texture discrimination, achieving improved performance over previous handcrafted methods. In this paper, we present a new approach that combines a learning technique and the Complex Network (CN) theory for texture analysis. This method takes advantage of the representation capacity of CN to model a texture image as a directed network and uses the topological information of vertices to train a randomized neural network. This neural network has a single hidden layer and uses a fast learning algorithm, which is able to learn local CN patterns for texture characterization. Thus, we use the weights of the trained neural network to compose a feature vector. These feature vectors are evaluated in a classification experiment in four widely used image databases. Experimental results show a high classification performance of the proposed method when compared to other methods, indicating that our approach can be used in many image analysis problems.

Keywords Randomized neural networks · Network science · Texture · Image classification

1 Introduction

Texture is a key visual feature used to describe images in many problems of computer vision and image processing such as plant recognition, medical image analysis, industrial inspection, and microscope images. The visual texture is composed of sub-patterns related to the pixel distribution and with certain similarity on the image [19]. Although it can be easily understood by the humans, there is no formal definition for the texture attribute. However, this fact did not prevent the progress and development of new approaches for texture analysis.

Many techniques for texture analysis have been proposed in the last decades. They can be divided into four classical categories according to the way of exploiting the texture characteristics of the image. The statistical-based approaches have been the most studied over the last decades. Examples of these approaches are the variants of Gray-Level Co-occurrence Matrices (GLCM) [24] and Local Binary Patterns (LBP) [37]. The structural approaches treat the image as an arrangement of textons (ie. small elements), which form the texture from a spatially organized pattern. Some methods of this kind of analysis are the Morphological decomposition [30] and key point detectors and descriptors to represent the texture elements [31]. On the other hand, in the spectral-based approaches, the image is exploited in the power spectrum domain and the most popular methods are the Gabor filters [34] and Wavelet transforms [13]. Finally, in the model-based approaches, the textures are represented using mathematical models and estimation of their parameters such as Fractal models [3, 46] and stochastic models [39].

More recently, innovative methods have been proposed to characterize textures, achieving promising results. In particular, methods that use learning techniques to represent the texture have gained prominence such as that ones based on a vocabulary of Scale Invariant Feature Transform (SIFT) [12] (called Bag-Of-Visual-Words (BOVW)), randomized neural networks [47, 48] and deep convolutional neural networks [7, 50–52]. On the other hand, methods based on

image complexity analysis have also gained attention due to its capacity to deal with the complex texture patterns. In this sense, one of the most popular are the methods based on Complex Network (CN) theory. These methods are very promising because of its ability to represent the relationships among structural elements of texture. However, once the textures are modeled as CNs, how to characterize it in order to obtain representative descriptors is a challenge to overcome.

In this paper, we propose to use a randomized neural network to learn and characterize the topology of a directed CN that models a texture image. Firstly, the image is modeled as a directed CN mapping the pixels into vertices and connecting the vertices based on a connection rule. For characterization, we use each vertex of the CN as a label and the neighboring vertices (ie. the eight neighboring pixels in a window 3×3) as an input vector for training a randomized neural network. A randomized neural network has a single-hidden layer with a very fast learning algorithm that can learn and characterize the topological characteristics of the CN. Thus, the feature vector of texture is composed of the output weights of a trained randomized neural network. In relation to the previous approach [45], the main contribution of this approach is a new way to build the label and input vectors to train the randomized neural network. The proposed approach is faster and improves the classification performance.

This paper is organized as follows. Section 2 describes the fundamentals of complex network theory and randomized neural network. The proposed method for texture analysis is described in Section 3. Experimental setup used in this work is presented in Section 4. The experimental results, discussion and comparison on four databases are presented in Section 5. Finally, Section 6 concludes the paper and suggests future works.

2 Background

2.1 Complex Networks

The Complex Network (CN) research, also called Network Science, arises from the combination between the graph theory, physics and statistics, targeting large and complicated real systems. Basically, most of these systems can be modeled as a structure composed of elements that interact with each other, which in a network are described by vertices and edges. However, the mathematical properties that governs these networks internal behavior is not trivial, as an example one can imagine the structural organization and functioning of the internet, composed of countless routers and computers (vertices) and their physical connections through wires (edges). These systems are collectively called complex systems, capturing the fact that it is difficult to derive their collective behavior from a knowledge of the system's components [5]. Initially, it was believed that most of the real networks had random topology [15, 16]. Further research then has shown various structural patterns, which led to the definition of network models such as the scale-free [6] (power-law-like degree distribution) and the small-world [54] (short average path distance and high vertex inter-connectivity). These phenomena were observed in several real systems, which then allowed important advances in the study of their functioning. Therefore, the complex network approach became popular on the analysis of various real systems in areas such as physics, biology, sociology and many more.

A Complex Network is usually defined by a combination of two sets, its vertices and edges. Let us define $V = \{v_1, \dots, v_n\}$ as a set of n vertices and $E = \{e_{v_i, v_j}\}$ as a set of m edges connecting vertex pairs, then a network is defined by $N = (V, E)$. Here we will focus on directed weighted networks, which implies that $e_{v_i, v_j} \neq e_{v_j, v_i}$ and $e_{v_i, v_j} \in \mathbb{R}$. To analyze a system from a network perspective, the first step is the modelling, which means defining the vertices and edges. Once the network N is built, several topological measures can be obtained to describe its structure [11]. One of the most traditional measures is the vertex degree, that counts the number of connections of a vertex

$$k_{v_i} = \sum_{\forall v_j \in V} \begin{cases} 1, & \text{if } e_{v_i, v_j} \in E \\ 0, & \text{otherwise} \end{cases} \quad (1)$$

In a directed network scenario, Equation 1 describes the output degree of vertex v_i , i.e. the number of connections leaving v_i . It is also possible to compute the input degree by inverting the verification from "if $e_{v_i, v_j} \in E$ " to "if $e_{v_j, v_i} \in E$ ". The traditional degree measure does not take into consideration the edge weights, therefore it is possible to calculate the weighted degree, also known as strength of a vertex

$$ks_{v_i} = \sum_{\forall v_j \in V} \begin{cases} e_{v_i, v_j}, & \text{if } e_{v_i, v_j} \in E \\ 0, & \text{otherwise} \end{cases} \quad (2)$$

which can also be computed for input connections, which we will denote ke_{v_i} . From the degree and strength of the vertices, many network properties can be quantified like its wiring patterns, the existence of the scale-free phenomenon, the identification of hubs and influent vertices, etc.

2.2 Randomized Neural Network

Randomized neural networks [26, 40, 41, 49] are artificial neural nets, which, in their simplest version, have a single hidden layer, whose weights are determined randomly, and an output layer whose weights can be determined using a closed-form solution. When these neural networks allow direct links between the input feature vectors and the output layer [40, 41], they are known as random vector functional link (RVFL) nets.

To mathematically explain a randomized neural network without direct links, let $X = [\vec{x}_1, \vec{x}_2, \dots, \vec{x}_N]$ be a set of N input feature vectors, each one having $p + 1$ attributes (each vector has an additional fixed value +1 for bias). Next, these input vectors can be processed by the hidden neurons by using $Z = \phi(WX)$, where $\phi(\cdot)$ is a transfer function and W is a matrix of weights of the hidden neurons whose dimensions are $Q \times (p + 1)$, where Q is the number of neurons of the hidden layer.

The matrix $Z = [\vec{z}_1, \vec{z}_2, \dots, \vec{z}_N]$ represents the outputs of the hidden layer for all input feature vectors, that is, $\vec{x}_i \rightarrow \vec{z}_i$. This matrix, after the inclusion of an additional fixed value +1 for bias in each vector, can be used to compute the weights of the output layer, according to

$$M = DZ^T(ZZ^T)^{-1}, \quad (3)$$

where $D = [\vec{d}_1, \vec{d}_2, \dots, \vec{d}_N]$ is a matrix of labels (each \vec{d}_i corresponding to its respective input vector \vec{x}_i) and $Z^T(ZZ^T)^{-1}$ is the Moore-Penrose pseudo-inverse [35, 43].

Sometimes, the square matrix ZZ^T is near-singular, resulting in unstable results for the matrix M . To solve this, it is possible to use the Tikhonov regularization [9, 53], as follows

$$M = DZ^T(ZZ^T + \lambda I)^{-1}, \quad (4)$$

where I is an identity matrix $(Q + 1) \times (Q + 1)$ and λ is a regularization parameter ($0 < \lambda < 1$).

3 Proposed Method

In this section, we describe the proposed method in detail, from the image modeling as a directed complex network to the characterization through learning local topological properties with randomized neural networks.

3.1 Modeling Texture as Directed Networks

Most of previous works approaching texture as Complex Networks considers each image pixel as a network vertex, and connections are based on their intensity similarity and spatial proximity. This is achieved through two modeling parameters: a radius, which defines a distance limit for connections, and a threshold for connection cutting. On the other hand, we employ a directed modeling as introduced in [45], where only the radius is needed, removing the need of finding ideal threshold values. Consider I as the input image with pixels $I(i) \in [0, L]$, where L defines the maximum intensity value of pixels, usually 255 for 8-bit images. A network $N^r(V, E)$ is built where $V = \{v_i\} \forall i \in I$ represent vertices, which maps each image pixel, and $E = \{e_{v_i, v_j}\}$ represent edges, connecting pairs of vertices. To create directed connections each vertex/pixel is centered in a sliding window of radius r and edges points in the direction of the gradient, i.e. towards pixels of higher intensity

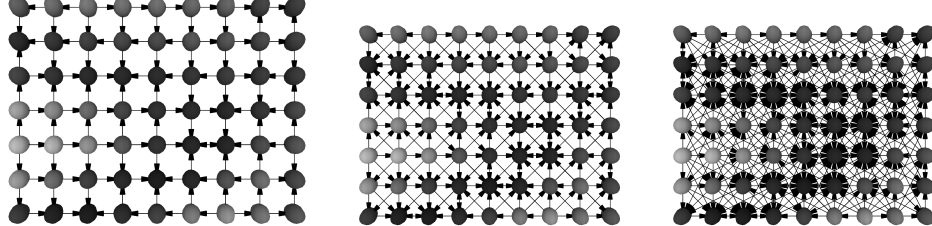
$$E = \{e_{v_i, v_j} \in E \mid d(v_i, v_j) \leq r \wedge I(i) < I(j)\} \quad (5)$$

where $d(v_i, v_j)$ represents the Euclidean distance between pixels i and j . If the pixel intensity is equal, the edge is bidirectional.

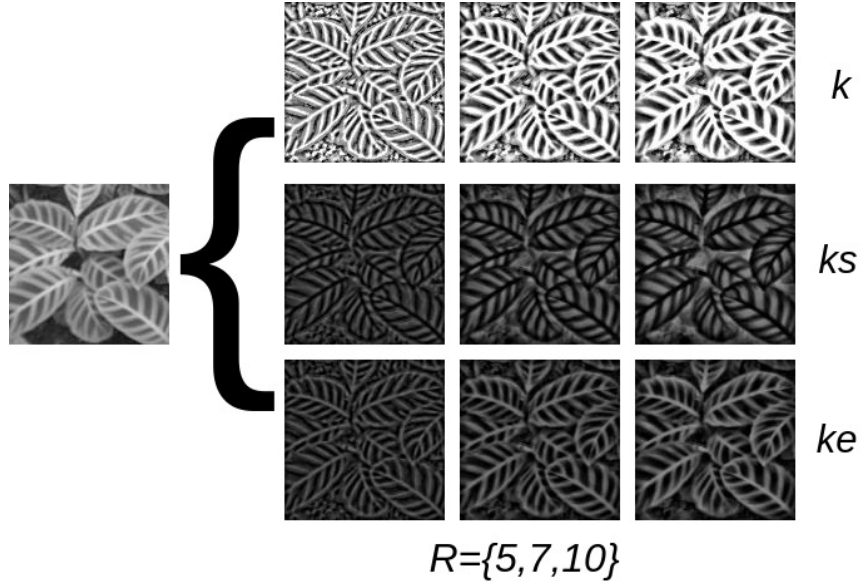
The connection weight plays an important role in the network structure, and it is crucial for computing the vertex strength. It is defined as a combination between the intensity difference and the spatial position of the pixels

$$e_{v_i, v_j} = \begin{cases} \frac{|I(i) - I(j)|}{L}, & \text{if } r = 1 \\ \frac{\left(\frac{d(v_i, v_j)-1}{r-1}\right) + \left(\frac{|I(i) - I(j)|}{L}\right)}{2}, & \text{otherwise.} \end{cases} \quad (6)$$

where $r = 1$ is the smallest possible distance, thus we consider only the intensity information. This equation yields an edge distribution normalized in the range $[0, 1]$, giving equal weight to both the intensity and the spatial position of the pixels. By varying the radius parameter r , it is possible to control the network density, i.e. as r increases, the number of connections increases. With a set of radii $R\{r_1, \dots, r_n\}$, different networks N^1, N^2, \dots, N^n can be modeled where one can analyze the dynamic evolution of the system (image), which is related to the interplay between neighbour pixels and, therefore, contains multiscale texture information. Figure 1(a) illustrates the structure of the directed network modeled for different values of r .



(a) Directed network structure for $R = \{1, 2, 3\}$.



(b) Visual representation of network measures.

Figure 1: The structure of directed complex networks (a) and a visual representation of different vertex measures obtained from networks modeled with the input image.

To quantify the network structure, three centrality measures are employed just as in [45], which are the output degree, input and output weighted degree (or strength). The out-degree k_{v_i} of a vertex v_i is computed by Eq. 1 and counts the number of vertices that v_i points. On the other hand, the weighted out-degree ks_{v_i} considers the weight of each connection leaving v_i . The weighted in-degree ke_{v_i} is then the opposite of the out-degree, i.e. it sums the edges that points to v_i ,

$$ke_{v_i} = \sum_{\forall v_j \in V} \begin{cases} e_{v_j, v_i}, & e_{v_j, v_i} \in E \\ 0, & \text{otherwise.} \end{cases} \quad (7)$$

Figure 1(b) shows a visual representation of the network measures computed for a given image texture for different radii, where pixels are obtained normalizing each measure by the maximum possible vertex degree. It is possible to notice that each topological measure represents a different local pattern related to the image intensity variation. The combination of these measures in a multiscale fashion provides rich texture information that we exploit to train neural networks to produce image descriptors. More details are given in the following section.

3.2 Learning Local Complex Features

The proposal of this paper is to use the randomized neural network to learn the main topological characteristics of a CN and then use the weights of the output layer of the trained RNN as a signature to represent the CN (ie. the texture). To achieve this, for each vertex of the CN, three information were considered: out-degree, weighted out-degree and weighted in-degree. As the out-degree is directly related to the in-degree in the modeled networks (i.e., the sum of the two degrees produces the same value in all vertices) and therefore have the same information, only the out-degree was considered.

In this method, we propose to apply windows of size 3×3 over the modeled network in order to build the matrix of input feature vectors for the randomized neural network. For this, firstly, consider that the Cartesian coordinates x_i and y_i of a vertex v_i are the same of the pixel i that is represented by the vertex. Thus, the window is the spatial neighborhood of a vertex based on the Cartesian coordinates. In other words, we divided the image into 3×3 joint windows, however, instead of using information directly from the pixels we use the information of the vertices that represent them (ie. from the CN). Figure 2 illustrates a window with a central pixel i represented by the vertex v_i and neighboring pixels represented by their vertices. Regarding this window, for each vertex v_i , the out-degree k_{v_i} is considered the label and the out-degrees of the neighboring vertices compose the input feature vector $\vec{x}_{v_i} = [k_{v_1}, k_{v_2}, k_{v_3}, \dots, k_{v_8}]$. This strategy to define the input feature vectors and the labels to train the neural network is the main difference between this approach and the previous work [45]. In the proposed approach, it is possible to compute the feature vector using a unique value of radius R for modeling, while in the previous work is necessary to use a set of values of radius to obtain a feature vector, increasing the computational time. In addition, in the proposed approach, instead of using the gray-level we use the out-degree as the label. Thus, the input feature vector and label are composed only of information from the CN.

v_1	v_2	v_3
v_8	v_i	v_4
v_7	v_6	v_5

Figure 2: Neighborhood of a vertex.

Figure 3(a) shows how the input feature vector and its respective label are obtained from a given vertex using a window 3×3 . A matrix of input feature vectors $X_{(k)}$ and a matrix of labels D for the out-degree are then constructed considering all the vertices of the network. Thus, it is possible to analyze the characteristics of the vertices that represent the pixels. In addition to the matrix of input feature vector $X_{(k)}$ containing the out-degree, we also construct matrices of input vectors using the weighted out-degree $X_{(ks)}$ and the weighted in-degree $X_{(ke)}$.

To train a randomized neural network, it is necessary to define the matrix of weights W of the hidden neurons. Generally, this matrix is randomly defined at each new training, changing also the values of the trained output weights. However, in feature extraction techniques it is important that the signature values be always equal for the same sample. Therefore, it is important to use the same values in the matrix of weights W to obtain the same signature for the same network. In this way, we used the same procedure adopted in [47] to obtain the pseudorandom uniform numbers for the matrix W , that is, the linear congruent generator (LCG) [42], according to

$$V(n+1) = (a * V(n) + b) \bmod c, \quad (8)$$

where V is the random sequence and the values a , b and c are parameters set up as $a = E + 2$, $b = E + 3$ e $c = E^2$ (values adopted in [47]), where $E = Q * (p + 1)$ is the length of the sequence V that is started by $V(1) = E + 1$. Thus, the matrix W is defined using the sequence V divided into Q segments of values $p + 1$. The matrices W and X (each row) are normalized to zero mean and unit variation.

The descriptors of the modeled CN and, consequently, the signature of the texture is obtained based on the matrix M , which is composed of the learned weights of the output layer. This one becomes a vector $\vec{f} = DZ^T(ZZ^T + \lambda I)^{-1}$, where $\lambda = 10^{-3}$, as illustrated in Figure 3(b). Notice that \vec{f} has a length $Q + 1$ due to the bias value. Thus, the first

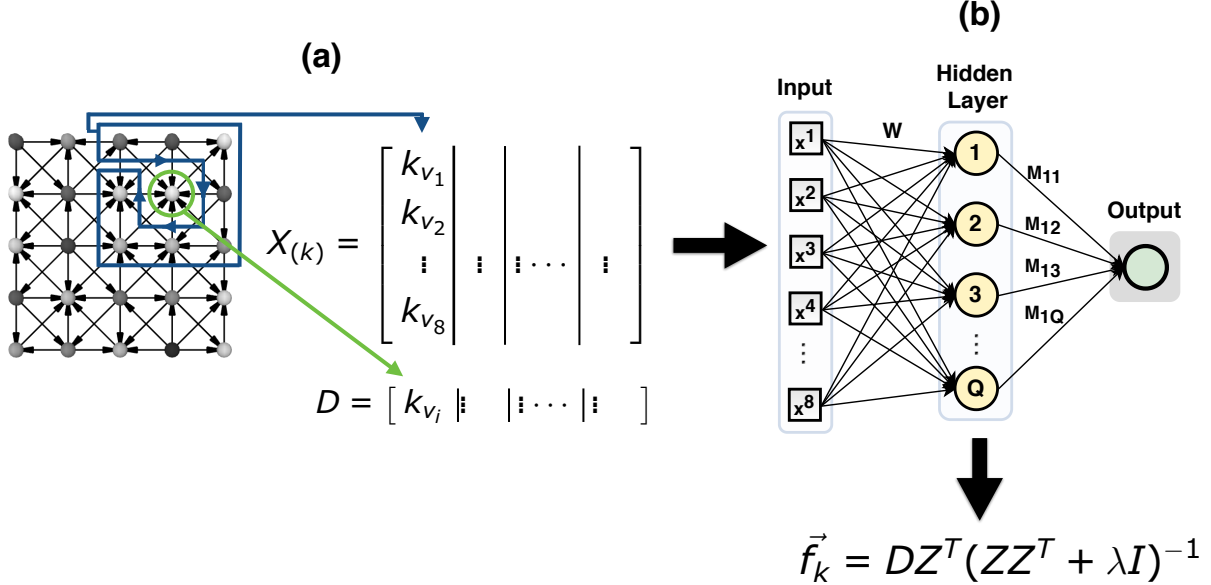


Figure 3: Label and input vector obtained from a network.

signature for a texture is obtained by concatenating the vectors \vec{f} of three RNNs trained with the three matrices of input feature vectors $X_{(k)}, X_{(k)}, X_{(k)}$,

$$\vec{\Upsilon}(Q)_r = [\vec{f}_k, \vec{f}_{ks}, \vec{f}_{ke}], \quad (9)$$

where Q is the number of hidden neurons and r is the radius to construct the CN. The signature $\vec{\Upsilon}(Q)_r$ is constructed using an unique value of Q and r . These two parameters influence the trained weights of the neural network and, therefore, provide different descriptors for different values. Taking advantage of this, we propose a signature $\vec{\Theta}(R)_{(Q_1, Q_2, Q_m)}$, which concatenates the vectors $\vec{\Upsilon}(Q)_r$ for different values of radius r ,

$$\vec{\Theta}(Q)_{r_1, r_2, \dots, r_m} = [\vec{\Upsilon}(Q)_{r_1}, \vec{\Upsilon}(Q)_{r_2}, \dots, \vec{\Upsilon}(Q)_{r_m}]. \quad (10)$$

Finally, a signature $\vec{\Psi}_{Q_1, Q_2, \dots, Q_n}$ which combines the vector $\vec{\Theta}(Q)_{r_1, r_2, \dots, r_m}$ using different values of Q is proposed, according to

$$\vec{\Psi}_{Q_1, Q_2, \dots, Q_n} = [\vec{\Theta}(Q_1)_{r_1, r_2, \dots, r_m}, \vec{\Theta}(Q_2)_{r_1, r_2, \dots, r_m}, \dots, \vec{\Theta}(Q_n)_{r_1, r_2, \dots, r_m}]. \quad (11)$$

4 Experimental Setup

To assess the performance of the proposed method, the following databases were evaluated:

- Brodatz [8]: just as in [4], we used 111 classes, 16 images of 128×128 pixels per class, totaling a data set of 1776 images.
- Vistex [44]: this data set is provided by the MIT Media Laboratory. Just as in [4], we used 54 classes, each one represented by an image 512×512 pixels divided into non-overlapping images of 128×128 pixels. Thus, the database has 16 images per class, thus resulting in a total of 864 images.
- Outex [36]: this framework provides several texture benchmark data sets, and, among them, we chose TC_Outex_00013, which is composed of 68 classes. Just as in [4], each class is represented by an image of 746×538 pixels, from which 20 images of 128×128 pixels were cropped without overlapping. Thus, the database used in this work has 1360 images.

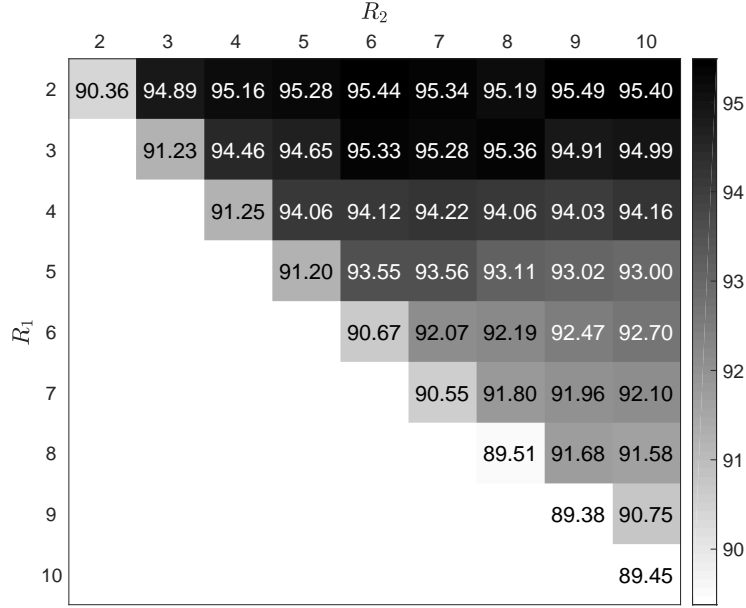


Figure 4: Accuracies of the signature $\vec{\Theta}(Q)_{R_1, R_2, \dots, R_m}$ using $Q = 4$ for different values of R on the four databases.

- USPTex [3]: this database is composed of 191 classes, 12 images per class, resulting in 2292 images, which represent a wide variety of scenes of everyday life, such as bark, sand, bricks, vegetation, sidewalk etc.

All color texture data sets were converted into grayscale. To classify the proposed signature, we used Linear Discriminant Analysis (LDA) [55]. This statistical method aims to project the data in order to maximize the distance inter-classes and minimize the variance within the same class. To validate the classification procedure, we used the *leave-one-out cross-validation* approach, which basically separates one sample for test, uses the remainder for training, and repeats this process N times (N is the number of samples), each time with a different sample for test. The validation performance is the mean accuracy of the N runs.

5 Results and Discussion

5.1 Parameter Analysis

In this section, we perform an evaluation of the parameters of our method in terms of accuracy on the four databases. The first signature analyzed is the $\vec{\Theta}(Q)_{R_1, R_2, \dots, R_m}$ with $Q = 4$. For this signature, different values of $R = \{2, 3, 4, 5, 6, 7, 8, 9, 10\}$ and their combinations were analyzed. The results are summarized in Figure 4, which presents the mean of the accuracies obtained in the four databases. In this experiment, a maximum of two values of R was combined due to the large number of characteristics generated for larger combinations.

The results indicate that for a single value of R (main diagonal of the matrix), the best result is reached with $R = 4$. However, it is clear that a single value of R yields results lower than that of the combination of two values of R . In this case, note that the best results are obtained when combining a low R value with a high R value (best result of 95.46% for $R = \{2, 9\}$). The values of R determine the radius of the network modeling, that is, for low R values the pixels are connected with nearest neighbors (local analysis), whereas for high R values, a global analysis of texture is performed. Thus, the combination of local and global characteristics is expected to provide superior results.

A second experiment to evaluate the feature vector $\vec{\Psi}_{Q_1, Q_2, \dots, Q_n}$ was performed. In this experiment, different values of $Q = \{04, 09, 14, 19, 24, 29\}$ were used for $r = \{2, 9\}$. Figure 5 shows the accuracies with the signature $\vec{\Psi}_{Q_1, Q_2, \dots, Q_n}$ on the four databases with different values of Q and their combinations. Note that the lower results are on the main diagonals, that is, when a single value of Q is considered. On the other hand, when two values of Q are considered, the accuracy increases. Table 1 shows the results for the combination of three values of Q . Note that higher accuracies

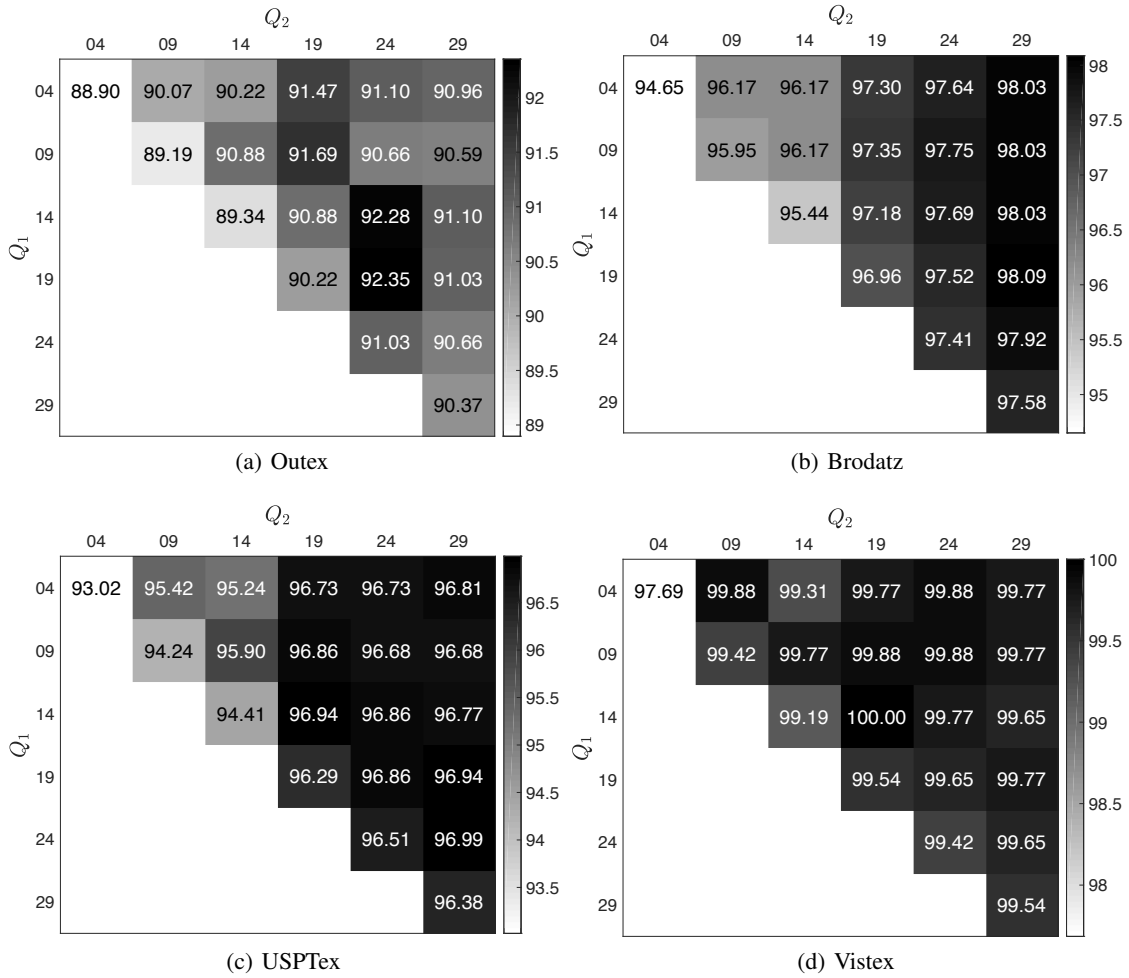


Figure 5: Accuracies of the feature vector $\vec{\Psi}_{Q_1, Q_2, \dots, Q_n}$ using different values of Q on the four databases.

were obtained with these combinations. However, as larger values of Q are combined, the size of the feature vector also increases and the accuracy tends to decrease or stabilize. Thus, we consider the vector $\vec{\Psi}_{04, 19, 29}$, which presents a good balance between accuracy and number of features on the four databases.

5.2 Comparison with other methods

In order to evaluate the results obtained by the proposed method, comparisons were performed with other methods of the literature. The experimental configurations were the same as described above, with the exception of the CLBP method, which used the classifier 1-Nearest Neighborhood (1-NN) with the distance chi-square according to the original paper. For the proposed method, the signature that obtained the best result in the previous analysis was considered: $\vec{\Psi}_{04, 19, 29}$.

We also compare the performance of our descriptor with deep convolutional neural networks, which are applied in a transfer-learning approach where a pre-trained architecture is used as feature extractor by computing the Global Average Pooling (GAP) [32] over the output of its last convolutional layer. The weights of these models are learned from the ImageNet dataset [14], composed of millions of images, and can be ported to various applications, such as texture analysis [10]. We considered four well-known models from the literature, the VGG19 (2014) [50], InceptionV3 (2016) [52], ResNet50 (2016) [25] and InceptionResNetV2 (2017) [51]. All models and their pre-trained weights were imported from the Keras 2.2.4 library¹. For these methods, the images are normalized by the maximum possible gray-level before being processed.

¹www.keras.io/applications

Table 1: Results for the feature vector $\vec{\Psi}_{Q_1, Q_2, \dots, Q_n}$ combining three values of Q .

Q	No of features	Outex	Brodatz	USPTex	Vistex
{04, 09, 14}	180	91.69	96.45	96.29	99.77
{04, 09, 19}	210	91.76	97.41	96.99	100.00
{04, 09, 24}	240	91.25	97.75	96.77	99.88
{04, 09, 29}	270	91.10	98.20	97.12	99.88
{04, 14, 19}	240	91.76	97.52	96.90	99.88
{04, 14, 24}	270	91.99	98.03	96.94	99.77
{04, 14, 29}	300	91.10	98.37	96.86	99.77
{04, 19, 24}	300	92.43	97.97	97.08	99.77
{04, 19, 29}	330	92.13	98.09	97.21	99.88
{04, 24, 29}	360	90.96	97.97	96.94	99.65
{09, 14, 19}	270	91.91	97.47	97.12	100.00
{09, 14, 24}	300	91.25	97.80	97.21	99.77
{09, 14, 29}	330	91.10	98.31	97.16	100.00
{09, 19, 24}	330	91.47	97.92	97.16	99.77
{09, 19, 29}	360	91.84	98.25	97.16	99.88
{09, 24, 29}	390	90.74	97.97	97.03	99.77
{14, 19, 24}	360	91.91	97.92	97.25	99.77
{14, 19, 29}	390	91.99	98.03	97.29	99.88
{14, 24, 29}	420	91.18	97.92	97.16	99.77
{19, 24, 29}	450	91.10	97.86	97.03	99.54

Table 2 presents the results obtained by our method and the others on the four texture databases. The results show that the proposed method obtained the best results when compared to the others on three databases (Outex, USPTex and Vistex). In relation to the methods based on convolutional neural networks, the ResNet50 model outperformed the proposed method only on the Brodatz database. On this database, all other approaches based on convolutional neural networks achieved higher results. However, it is possible to note that these methods did not have a good performance on the Outex database, which is characterized by samples with different illuminations.

It is also important to highlight that the proposed method improved the accuracy when compared to the ELM Signature and CNDT method (which are based on neural network nets and complex networks, respectively). The ELM Signature method uses only the pixel intensities to train the RNNs and characterize the textures, which shows that modeling in CNs and their topology are important in texture analysis. On the other hand, the CNDT method models the images in complex networks and calculates traditional measures of CN to compose the feature vector. In this context, the results suggest that our approach of learning complex network characteristics using randomized neural networks to characterize textures is more discriminative.

6 Conclusion

This paper proposed a novel way of extracting information from complex networks to train randomized neural networks in order to use the weights of output neurons to compose a texture signature. Unlike the method proposed in [45], our approach proposed a different strategy to construct the input feature vector and the label, which is based on CN information only. This one uses a unique value of radius to model the complex network and train the neural network,

Table 2: Comparison of accuracies of different texture analysis methods in four texture databases.

Methods	No of features	Outex	USPTex	Brodatz	Vistex
GLCM [23]	24	80.73	83.63	90.43	92.24
GLDM [29]	60	86.76	91.92	94.43	97.11
Gabor Filters [27]	64	81.91	83.19	89.86	93.28
Fourier [1]	63	81.91	67.70	75.90	79.51
Fractal [2]	69	80.51	78.22	87.16	91.67
Fractal Fourier [17]	68	68.38	59.45	71.96	79.75
LOSIB [18]	8	57.50	56.61	64.64	67.71
LBP [37]	256	81.10	85.42	93.64	97.92
LBPV [22]	555	75.66	55.13	86.26	88.65
CLBP [21]	648	85.80	91.13	95.32	98.03
AHP [56]	120	88.31	94.89	94.88	98.38
BSIF [28]	256	77.43	77.48	91.44	88.66
LCP [20]	81	86.25	91.31	93.47	94.44
LFD [33]	276	82.57	83.59	90.99	94.68
LPQ [38]	256	79.41	85.29	92.51	92.48
ELM Signature [47]	180	89.70	95.11	95.27	98.14
CNTD [4]	108	86.76	91.71	95.27	98.03
CNRNN_1 [45]	180	91.54	96.64	96.11	98.73
CNRNN_2 [45]	240	91.32	96.94	96.06	99.19
VGG19 [50]	512	76.62	93.19	96.79	97.45
InceptionV3 [52]	2048	86.40	96.77	98.54	98.84
ResNet50 [25]	2048	65.66	62.30	81.98	81.71
InceptionResNetV2 [51]	1536	85.88	96.34	98.99	98.96
Proposed approach	330	92.13	97.21	98.09	99.88

decreasing the computational time. The success rates of our approach were very high, surpassing accuracies of a large set of compared methods, including some based on deep learning. Thus, in the light of the obtained results, we believe that our approach offers a relevant contribution to the novel and promising field of research that studies how to connect neural and complex networks to build image signatures.

Acknowledgment

Lucas Correia Ribas gratefully acknowledges the financial support grant #s 2016/23763-8 and 16/18809-9, São Paulo Research Foundation (FAPESP). Jarbas Joaci de Mesquita Sá Junior thanks CNPq (National Council for Scientific and Technological Development, Brazil) (Grant: 302183/2017-5) for the financial support of this work. Leonardo Scabini acknowledges support from CNPq (Grant number #142438/2018-9). Odemir M. Bruno thanks the financial support of CNPq (Grant # 307897/2018-4) and FAPESP (Grant #s 14/08026-1 and 16/18809-9). The authors are also grateful to the NVIDIA GPU Grant Program for the donation of the Quadro P6000 and the Titan Xp GPUs used on this research.

References

- [1] AZENCOTT, R., WANG, J.-P., AND YOUNES, L. Texture classification using windowed Fourier filters. *IEEE Transactions on Pattern Analysis and Machine Intelligence* 19, 2 (1997), 148–153.
- [2] BACKES, A. R., CASANOVA, D., AND BRUNO, O. M. Plant leaf identification based on volumetric fractal dimension. *International Journal of Pattern Recognition and Artificial Intelligence* 23, 06 (2009), 1145–1160.

[3] BACKES, A. R., CASANOVA, D., AND BRUNO, O. M. Color texture analysis based on fractal descriptors. *Pattern Recognition* 45, 5 (2012), 1984–1992. <http://scg.ifsc.usp.br/dataset/USPtex.php>.

[4] BACKES, A. R., CASANOVA, D., AND BRUNO, O. M. Texture analysis and classification: A complex network-based approach. *Information Sciences* 219 (2013), 168–180.

[5] BARABÁSI, A., AND PÓSFAI, M. *Network Science*. Cambridge University Press, 2016.

[6] BARABÁSI, A.-L., AND ALBERT, R. Emergence of scaling in random networks. *science* 286, 5439 (1999), 509–512.

[7] BASU, S., KARKI, M., MUKHOPADHYAY, S., GANGULY, S., NEMANI, R., DiBIANO, R., AND GAYAKA, S. A theoretical analysis of deep neural networks for texture classification. In *2016 International Joint Conference on Neural Networks (IJCNN)* (2016), IEEE, pp. 992–999.

[8] BRODATZ, P. *Textures: A photographic album for artists and designers*. Dover Publications, New York, 1966.

[9] CALVETTI, D., MORIGI, S., REICHEL, L., AND SGALLARI, F. Tikhonov regularization and the L-curve for large discrete ill-posed problems. *Journal of Computational and Applied Mathematics* 123, 1 (2000), 423 – 446.

[10] CIMPOI, M., MAJI, S., KOKKINOS, I., AND VEDALDI, A. Deep filter banks for texture recognition, description, and segmentation. *International Journal of Computer Vision* 118, 1 (2016), 65–94.

[11] COSTA, L. D. F., RODRIGUES, F. A., TRAVIESO, G., AND VILLAS BOAS, P. R. Characterization of complex networks: A survey of measurements. *Advances in Physics* 56, 1 (2007), 167–242.

[12] CSURKA, G., DANCE, C., FAN, L., WILLAMOWSKI, J., AND BRAY, C. Visual categorization with bags of keypoints. In *ECCV International Workshop on Statistical Learning in Computer Vision* (2004), pp. 1–22.

[13] DE VES, E., ACEVEDO, D., RUEDIN, A., AND BENAVENT, X. A statistical model for magnitudes and angles of wavelet frame coefficients and its application to texture retrieval. *Pattern Recognition* 47, 9 (2014), 2925 – 2939.

[14] DENG, J., DONG, W., SOCHER, R., LI, L.-J., LI, K., AND FEI-FEI, L. Imagenet: A large-scale hierarchical image database. In *Computer Vision and Pattern Recognition, 2009. CVPR 2009. IEEE Conference on* (2009), Ieee, pp. 248–255.

[15] ERDOS, P., AND RÉNYI, A. On random graphs i. *Publ. Math. Debrecen* 6 (1959), 290–297.

[16] ERDOS, P., AND RÉNYI, A. On the evolution of random graphs. *Publ. Math. Inst. Hungar. Acad. Sci* 5 (1960), 17–61.

[17] FLORINDO, J. B., AND BRUNO, O. M. Fractal descriptors based on Fourier spectrum applied to texture analysis. *Physica A: statistical Mechanics and its Applications* 391, 20 (2012), 4909–4922.

[18] GARCÍA-OLALLA, O., ALEGRE, E., FERNÁNDEZ-ROBLES, L., AND GONZÁLEZ-CASTRO, V. Local oriented statistics information booster (losib) for texture classification. In *Pattern Recognition (ICPR), 2014 22nd International Conference on* (2014), IEEE, pp. 1114–1119.

[19] GONÇALVES, W. N., DA SILVA, N. R., DA FONTOURA COSTA, L., AND BRUNO, O. M. Texture recognition based on diffusion in networks. *Information Sciences* 364 (2016), 51–71.

[20] GUO, Y., ZHAO, G., AND PIETIKÄINEN, M. Texture classification using a linear configuration model based descriptor. In *BMVC* (2011), Citeseer, pp. 1–10.

[21] GUO, Z., ZHANG, L., AND ZHANG, D. A completed modeling of local binary pattern operator for texture classification. *IEEE Transactions on Image Processing* 19, 6 (2010), 1657–1663.

[22] GUO, Z., ZHANG, L., AND ZHANG, D. Rotation invariant texture classification using lbp variance (lbpv) with global matching. *Pattern recognition* 43, 3 (2010), 706–719.

[23] HARALICK, R. M. Statistical and structural approaches to texture. *Proceedings of the IEEE* 67, 5 (1979), 786–804.

[24] HARALICK, R. M., SHANMUGAM, K., AND DINSTEIN, I. H. Textural features for image classification. *Systems, Man and Cybernetics, IEEE Transactions on*, 6 (1973), 610–621.

[25] HE, K., ZHANG, X., REN, S., AND SUN, J. Deep residual learning for image recognition. In *Proceedings of the IEEE conference on computer vision and pattern recognition* (2016), pp. 770–778.

[26] HUANG, G.-B., ZHU, Q.-Y., AND SIEW, C.-K. Extreme learning machine: theory and applications. *Neurocomputing* 70, 1 (2006), 489–501.

[27] IDRISIA, M., AND ACHEROY, M. Texture classification using Gabor filters. *Pattern Recognition Letters* 23, 9 (2002), 1095–1102.

[28] KANNALA, J., AND RAHTU, E. Bsif: Binarized statistical image features. In *Pattern Recognition (ICPR), 2012 21st International Conference on* (2012), IEEE, pp. 1363–1366.

[29] KIM, J. K., AND PARK, H. W. Statistical textural features for detection of microcalcifications in digitized mammograms. *IEEE transactions on medical imaging* 18, 3 (1999), 231–238.

[30] LAM, W.-K., AND LI, C.-K. Rotated texture classification by improved iterative morphological decomposition. *IEE Proceedings-Vision, Image and Signal Processing* 144, 3 (1997), 171–179.

[31] LAZEBNIK, S., SCHMID, C., AND PONCE, J. A sparse texture representation using local affine regions. *IEEE Transactions on Pattern Analysis and Machine Intelligence* 27, 8 (2005), 1265–1278.

[32] LIN, M., CHEN, Q., AND YAN, S. Network in network. *arXiv preprint arXiv:1312.4400* (2013).

[33] MAANI, R., KALRA, S., AND YANG, Y.-H. Noise robust rotation invariant features for texture classification. *Pattern Recognition* 46, 8 (2013), 2103–2116.

[34] MANJUNATH, B. S., AND MA, W.-Y. Texture features for browsing and retrieval of image data. *IEEE Transactions on pattern analysis and machine intelligence* 18, 8 (1996), 837–842.

[35] MOORE, E. H. On the reciprocal of the general algebraic matrix. *Bulletin of the American Mathematical Society* 26 (1920), 394–395.

[36] OJALA, T., MÄENPÄÄ, T., PIETIKÄINEN, M., VIERTOLA, J., KYLLÖNEN, J., AND HUOVINEN, S. Outex: New framework for empirical evaluation of texture analysis algorithms. In *International Conference on Pattern Recognition* (2002), pp. 701–706.

[37] OJALA, T., PIETIKAINEN, M., AND MAENPAA, T. Multiresolution gray-scale and rotation invariant texture classification with local binary patterns. *IEEE Transactions on pattern analysis and machine intelligence* 24, 7 (2002), 971–987.

[38] OJANSIVU, V., AND HEIKKILÄ, J. Blur insensitive texture classification using local phase quantization. In *International conference on image and signal processing* (2008), Springer, pp. 236–243.

[39] PANJWANI, D. K., AND HEALEY, G. Markov random field models for unsupervised segmentation of textured color images. *IEEE Transactions on pattern analysis and machine intelligence* 17, 10 (1995), 939–954.

[40] PAO, Y.-H., PARK, G.-H., AND SOBAJIC, D. J. Learning and generalization characteristics of the random vector functional-link net. *Neurocomputing* 6, 2 (1994), 163–180.

[41] PAO, Y.-H., AND TAKEFUJI, Y. Functional-link net computing: theory, system architecture, and functionalities. *Computer* 25, 5 (1992), 76–79.

[42] PARK, S. K., AND MILLER, K. W. Random number generators: good ones are hard to find. *Communications of the ACM* 31, 10 (1988), 1192–1201.

[43] PENROSE, R. A generalized inverse for matrices. *Mathematical Proceedings of the Cambridge Philosophical Society* 51, 3 (1955), 406—413.

[44] PICARD, R., GRACZYK, C., MANN, S., WACHMAN, J., PICARD, L., AND CAMPBELL, L. *Vision texture database*. Media Laboratory, MIT, Cambridge, Massachusetts, 1995.

[45] RIBAS, L. C., DE MESQUITA [SÁ JUNIOR], J. J., SCABINI, L. F., AND BRUNO, O. M. Fusion of complex networks and randomized neural networks for texture analysis. *Pattern Recognition* 103 (2020), 107189.

[46] RIBAS, L. C., GONÇALVES, D. N., ORUÊ, J. P. M., AND GONÇALVES, W. N. Fractal dimension of maximum response filters applied to texture analysis. *Pattern Recognition Letters* 65 (2015), 116–123.

[47] SÁ JUNIOR, J. J. M., AND BACKES, A. R. ELM based signature for texture classification. *Pattern Recognition* 51 (2016), 395–401.

[48] SÁ JUNIOR, J. J. M., BACKES, A. R., AND BRUNO, O. M. Randomized neural network based signature for color texture classification. *Multidimensional Systems and Signal Processing* 30, 3 (2019), 1171–1186.

[49] SCHMIDT, W. F., KRAAIJVELD, M. A., AND DUIN, R. P. W. Feedforward neural networks with random weights. In *Proceedings., 11th IAPR International Conference on Pattern Recognition. Vol.II. Conference B: Pattern Recognition Methodology and Systems* (1992), pp. 1–4.

[50] SIMONYAN, K., AND ZISSERMAN, A. Very deep convolutional networks for large-scale image recognition. *arXiv preprint arXiv:1409.1556* (2014).

[51] SZEGEDY, C., IOFFE, S., VANHOUCKE, V., AND ALEMI, A. A. Inception-v4, inception-resnet and the impact of residual connections on learning. In *Thirty-First AAAI Conference on Artificial Intelligence* (2017).

- [52] SZEGEDY, C., VANHOUCKE, V., IOFFE, S., SHLENS, J., AND WOJNA, Z. Rethinking the inception architecture for computer vision. In *The IEEE Conference on Computer Vision and Pattern Recognition (CVPR)* (June 2016).
- [53] TIKHONOV, A. N. On the solution of ill-posed problems and the method of regularization. *Dokl. Akad. Nauk USSR* 151, 3 (1963), 501—504.
- [54] WATTS, D. J., AND STROGATZ, S. H. Collective dynamics of ‘small-world’ networks. *nature* 393, 6684 (1998), 440–442.
- [55] WEBB, A. *Statistical Pattern Recognition*, 2nd ed. John Wiley & Sons Ltd, Chichester, England, 2002.
- [56] ZHU, Z., YOU, X., CHEN, C. P., TAO, D., OU, W., JIANG, X., AND ZOU, J. An adaptive hybrid pattern for noise-robust texture analysis. *Pattern Recognition* 48, 8 (2015), 2592–2608.